Acta of Bioengineering and Biomechanics
Vol. 16, No. 2, 2014

Original paper
DOI: 10.5277/abb140212

Contact mechanics and wear simulations of hip resurfacing devices using computational methods

MURAT ALI*, KEN MAO

School of Engineering, University of Warwick, Coventry, UK.

The development of computational and numerical methods provides the option to study the contact mechanics and wear of hip resurfacing devices. The importance of these techniques is justified by the extensive amount of testing and experimental work required to verify and improve current orthopaedic implant devices. As the demands for device longevity is increasing, it is as important as ever to study techniques for providing much needed orthopaedic hip implant solutions. Through the use of advanced computer aided design and the finite element method, contact analysis of hip resurfacing devices was carried out by developing both three-dimensional and two-dimensional axisymmetric models whilst considering the effects of loading conditions and material properties on the contact stresses. Following on from this, the three-dimensional model was used in combination with a unique programme to develop wear simulations and obtain cumulative wear for both the acetabular cup and femoral head simultaneously.

Key words: *archard wear law, biotribology, contact, finite element analysis, wear*

1. Introduction

The introduction of hip replacements inspired the development and production of hip resurfacing devices, which are designed to reduce the volumetric wear rates of the implant devices and increase the longevity of the implantation. These products are also aimed to be suitable for younger patients who require a hip joint implant. The study of wear and surface damage has long been of a high importance for hip implant research, development and manufacture. In the past, the majority of research was mainly focused on the use of experimental in vitro testing simulators to predict the mechanical wear of the implant devices using international standards. With the increasing demands on orthopaedic device companies to produce validated and reliable implants which are safe for patients, the necessity for new and improved techniques to be developed and support the engineering activities of such devices is imperative.

In addition to carrying out experimental simulator testing, a viable alternative method for studying the mechanical wear of hip resurfacing devices is through the development of computational contact and wear models which can predict the wear of hip resurfacing devices [1]. The complexity of wear mechanisms [2] makes modelling such problems more challenging than traditional stress and strain analysis using the finite element method. To reduce the complexity of modelling wear mechanisms, a number of wear models have been proposed in the past and the most widely used is the Archard wear model [3], which is still used today as shown by recent literature by Rońda and Wojnarowski [4].

The objective of this study was to model the contact mechanics of hip resurfacing devices under normal, edge loading and serve loading conditions, specifically assessing the contact stresses of the hip implant. Obtaining the contact stress results along with carefully assessing the boundary conditions and material properties applied, formed the basis for developing wear models which could be applied to as-

* Corresponding author: Murat Ali, School of Engineering, University of Warwick, Coventry, CV4 7AL, UK. Tel: +44 24 7652 8193, fax: +44 24 7641 8922, e-mail: murat.ali@warwick.ac.uk.

Received: July 19th, 2013
Accepted for publication: November 14th, 2013

sess the volumetric wear of both the femoral head and acetabular cup simultaneously, which has not been considered in previous literature.

2. Materials and methods

A three-dimensional segmented hip resurfacing device model and two-dimensional axisymmetric model were developed based on the models used for contact analysis by Ali and Mao [5], [6], with a cup and head bearing diameter of 50 mm and diametral clearance of 80 μm based geometrically on the models proposed by Udofia et al. [7]. The segmented model allowed for the use of DICOM (Digital Imaging and Communications in Medicine) bone scans to be prepared for an assembly with hip resurfacing implant models using Solidworks (Dassault Systèmes SolidWorks Corporation, Waltham, Massachusetts, USA)

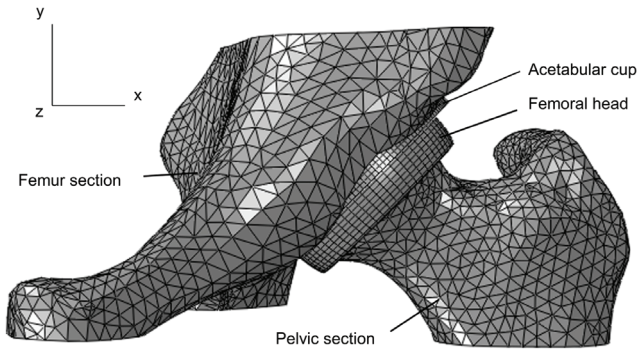

Fig. 1. Segmented three-dimensional hip resurfacing finite element model

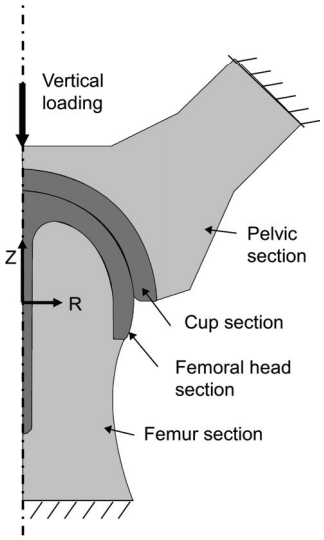

Fig. 2. Two-dimensional axisymmetric hip resurfacing finite element model

computer aided design. Through an associative interface with the commercially and academically available finite element analysis software Simulia ABAQUS (Version 6.10-1, Dassault Systèmes SolidWorks Corporation, Waltham, Massachusetts, USA), finite element assembly models were developed as shown in Fig. 1 and Fig. 2.

A combination of hexagonal (C3D8I) and wedge (C3D6) finite elements were used for modelling the acetabular cup and femoral head components. These elements were selected based on their suitability for studying the contact mechanics of hip implant devices. During the model meshing process, seeding techniques were used including definitions of part seed sizes and edge seeding with directional bias to define nodal points in areas of high contact stresses such as edge loading and rim contact. Due to the geometrical complexity of the femur and pelvic bone models, an automatic meshing algorithm was utilised and based on tetrahedral elements. A sliding contact interaction algorithm was defined with a nominal value of friction coefficient between the femoral head and acetabular cup of 0.16, which was based on the friction factor of CoCrMo on CoCrMo (cobalt chromium molybdenum) in both bovine serum and synovial fluid [8].

Following on from the development of the three-dimensional model, the two-dimensional axisymmetric model allowed for a computational efficient comparison of contact pressures and stresses of three different vertical loading conditions. The ISO vertical loading of 3000 N (F_I) and vertical load of 3900 N (F_y) were applied based on the peak load expected to occur during the walking cycle. In addition to this, a stumbling load of 11000 N (F_s) was also considered, as these high vertical loads have been highlighted to occur in vivo [9].

Both implicit and explicit finite element solvers were used to study the contact pressure during edge loading conditions and rim contact between the femoral head and acetabular cup. The use of the implicit solver allowed for an assessment of rim contact to be made under lateral sliding of the femoral head leading to edge loading rim contact. The explicit solver provided a suitable numerical method for studying the contact mechanics at the rim of the acetabular cup caused by inferior and lateral microseparation leading to edge loading. This type of edge loading contact occurs during the re-engagement of the femoral head within the acetabular cup as a result of vertical loading at heal strike which is referred to as “pure” microseparation in this study. The differences between both implicit and explicit techniques for engineering prob-

lem solving has been concisely explained by Harewood and McHugh [10]. For an implicit analysis, a system of equations are required to be solved for each analysis and displacement incrementation. The global stiffness matrix K can be inverted to solve for incremental displacements, however, this is very often a computationally intensive process, especially for non-linear quasi-static problems involving contact.

Modelling normal contact conditions and lateral displacement edge loading between the femoral head and acetabular cup was achieved by reaching incremental equilibrium using the implicit method based on the Newton–Raphson solver. For solving the finite element problem under laxity based edge loading the explicit method was utilised. For laxity based edge loading a microseparation distance between the femoral head and acetabular cup was first established, as this is expected to occur during swing phase of the human walking gait cycle. Following on from this, contact would occur under the action of the vertical load during the stance phase. This is a complex contact condition to model, therefore, a forward Euler integration scheme was used, which can be used to solve complex contact problems. Overall, the explicit analysis is less computational intensive than implicit modelling as large stiffness matrices are not required to be inverted.

In order to simulate wear based on the Archard Wear model, the magnitude of linear wear depth h_I given by

$$h_I = \sum_{i=1}^{n} k_w p_i (s_i - s_{i-1}) \tag{1}$$

was defined at each node as being linearly proportional to contact pressure p, sliding distance s and wear coefficient value k_w at each analysis increment i. The number of quasi-static finite element iterations were defined from $i = 1$ to n. Wear coefficients were assumed to be constant during bedding-in and steady state phases as observed from experimental hip simulator studies, with the same approach applied within previous wear simulation models [1].

The gait loading boundary conditions have been applied based on the ISO (International Organisation of Standardization) standards developed for in vitro testing, which simulate typical walking gait loading profiles as discussed by Bergmann [11]. This causes contact to occur between the hip implant bearing components. The sliding distance is determined by the physical sliding between the bearing components in contact, which occur through the relative angular displacement of the bearing. Therefore, ISO standard flexion-extension and inward-outward rotations are modelled as kinematic boundary conditions.

To calculate the sliding distance between the implant devices, two numerical methods were used through a combination of the finite element output database and user defined interfaces. One of the methods involved calculating the magnitude of the relative sliding distance d between the two contact surfaces and the other was based on the change in coordinate position of the femoral head during the angular displacement cycle

$$d_i = \sqrt{(u_i - u_{i-1})^2 + (v_i - v_{i-1})^2 + (w - w_{i-1})^2} \tag{2}$$

where u, v and w are the displacements in the x, y and z direction. For both methods, the finite element iteration defined the intervals at which the sliding distance was calculated. Although the abduction-adduction angular displacement was not included in the contact sliding model due to modelling constraints, literature has shown the wear rates from the assessments of in vivo retrieval implants match wear rates from two-axis experimental simulator studies more closely than studies using three-axis simulators (three motion rig) [12]. All rotations have been applied about the centre point of the femoral head (Fig. 3), which was defined as the centre of rotation.

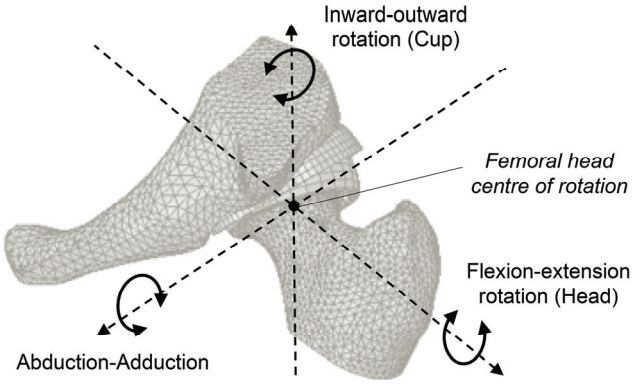

Fig. 3. Hip resurfacing contact and wear simulation model with angular displacements

The wear simulation method was developed using a Python scripting interface along with the finite element model. Following the calculation of linear wear at each increment, the total wear h_T is multiplied by the number of cycles k before finite element remeshing occurs

$$h_T = \sum_{i=1}^{k} h_I \ . \tag{3}$$

The total cumulative nodal linear and volumetric wear was calculated and the results presented. More detail on the wear simulation process is provided in Fig. 4. This is an alternative method to that previ-

ously developed by other researchers using subroutines to simulate wear. The material models and methodology for both the metal-on-metal CoCrMo hip bearing implants and bone models are discussed within a previous study by Ali and Mao [5]. A summary of the nominal materials model values are provided in Table 1, where E_F and E_P are the equivalent elastic modulus values applied to the femur and pelvic bone models, respectively.

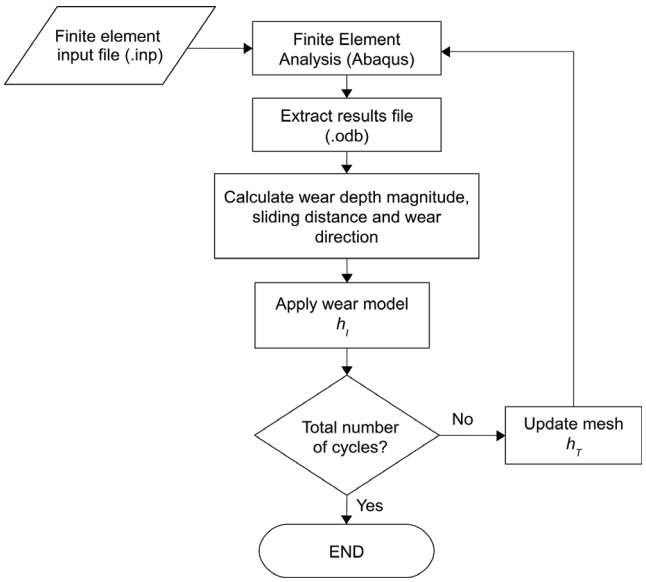

Fig. 4. Python scripting wear simulation procedure

Table 1. Material properties for finite element modelling

Material	Elastic modulus (GPa)	Poisson's ratio	Density (kg/m^3)
E_F	12.3	0.30	1900
E_P	6.1	0.30	1900
CoCrMo	230	0.30	8270

In addition to establishing isotropic and homogeneous material properties for the pelvic and femur bone sections, more complex orthotropic and Hounsfield based density greyscale material models were also modelled. For the greyscale model, each finite element was defined with a value of density (ρ). Therefore, Poisson's ratio (v) and Young's modulus (E) were defined as a function of density. The Hounsfield unit (GS) is determined from

$$GS = 1000 \times \frac{\mu_x - \mu_{\text{water}}}{\mu_{\text{water}}} \tag{4}$$

where the linear attenuation of water is given by μ_{water} and the coefficient of the substance being measured is given by μ_x. The density and Young's modulus values are determined from definition of the user defined coefficients a_j, b_j, c_j and d_j where j denotes the subscripts a, b and c

$$\rho = a_a + b_a GS\,, \tag{5}$$

$$\begin{bmatrix} v \\ E \end{bmatrix} = \begin{bmatrix} a_b & b_b + d_b & 0 \\ a_c & 0 & b_c + d_c \end{bmatrix} \begin{bmatrix} 1 \\ \rho^{c_b} \\ \rho^{c_c} \end{bmatrix}. \tag{6}$$

To determine if obtaining an equivalent modulus values for each patient specific scanned femur model and pelvic model should be repeated, a parametric study was carried out by varying bone elastic modulus values. Firstly, the same elastic modulus was applied to both the femur and pelvis, this was varied between 3 GPa to 25 GPa. Then a separate segmented bone model was assembled with the femoral head and acetabular cup components, the elastic modulus was varied independently between values of 3 GPa and 30 GPa. This provided an assessment for the relative material properties of the femur and pelvic bone models. By carrying out this analysis, the effect of bone material properties on the contact pressures and stresses were assessed.

3. Results

3.1. Contact mechanics of normal, edge loading and severe loading conditions

The variation of maximum contact pressure, von Mises stress and principal stress against the femur and pelvic bone elastic modulus is provided in Fig. 5. A relative bone elastic modulus was applied between the femur and pelvis, the contact pressure and von Mises stresses are shown in Fig. 6. Along with change of contact pressure caused by different values of elastic modulus, any difference in contact pressure magnitude between the two graphs was also due to the development of the segmented model being repeated to check for any model errors, and assess the sensitivity of the geometry and assembly differences on the contact pressure and stress results. Although both three-dimensional segmented hip implant models were based on the same DICOM bone model data, loading conditions and implant devices, there was a difference

of 15º anteversion angle between the models, however, it was observed that the difference in contact pressure distribution for each of the models was negligible, therefore detailed pressure and stress distribution plots are not provided.

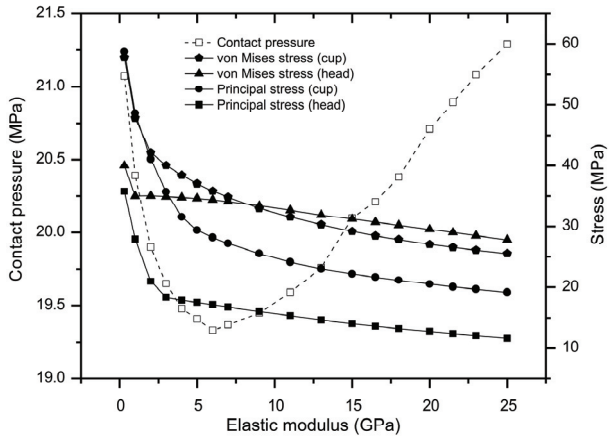

Fig. 5. Maximum contact pressure and stress against bone elastic modulus

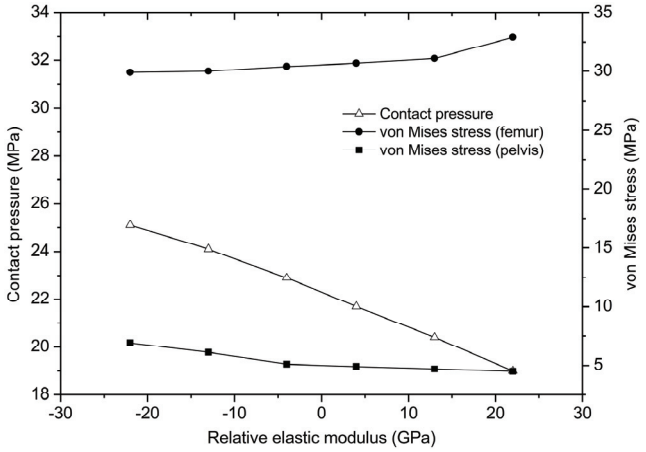

Fig. 6. Maximum contact pressure and von Mises stress against relative bone elastic modulus

By applying an orthotropic bone model, an assessment was conducted to obtain the contact pressure and von Mises stresses based on the material properties defined by Couteau et al. [13]. The percentage contact pressure difference as the relative elastic modulus was varied is shown in Fig. 7. The range of elastic modulus as presented from the study by Rho et al. [14] is highlighted on the graph. When applying the flexion-extension and inward-outward angular rotation to the three-dimensional finite element model along with the ISO gait loading conditions, the maximum von Mises stress, principal stress and three components of shear stress S12, S23 and S13 were plotted from the beginning to the end of one complete gait cycle (Fig. 8), as required for the implant volumetric wear analysis.

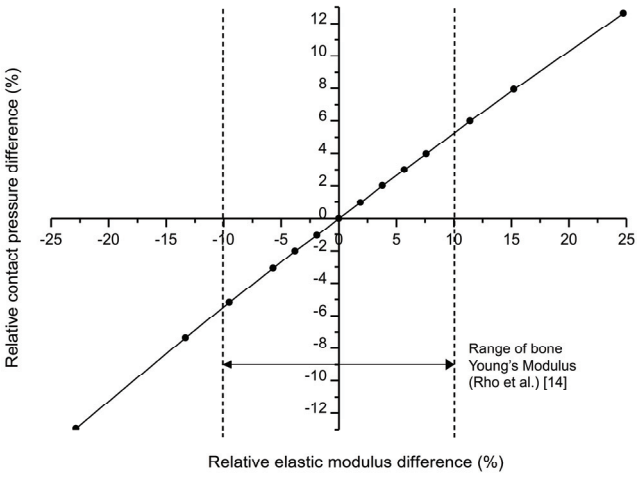

Fig. 7. Relative elastic modulus difference against relative contact pressure difference

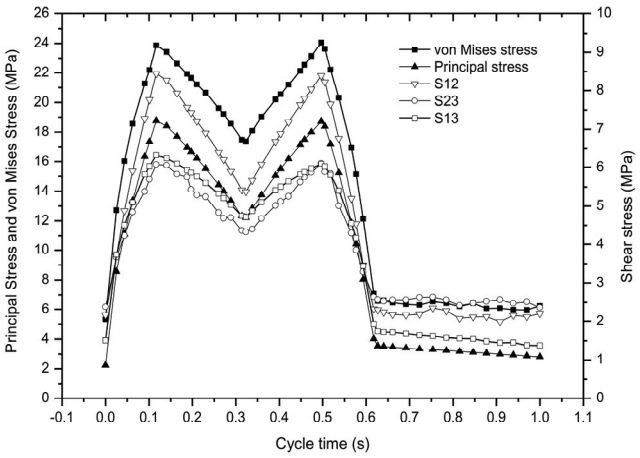

Fig. 8. Acetabular cup maximum principal stress, maximum von Mises stress and maximum shear stress with surface friction coefficient of 0.16

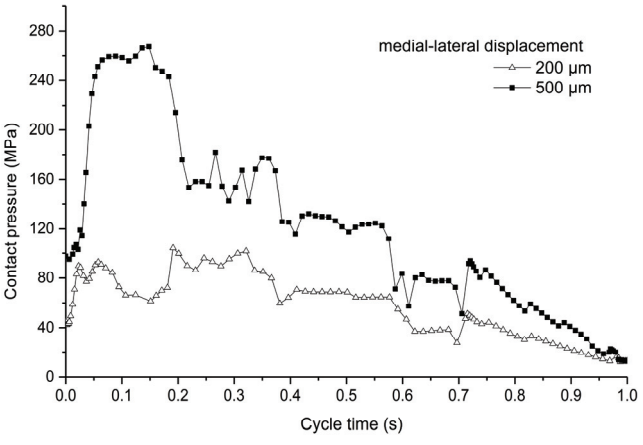

Fig. 9. Maximum contact pressure during loading cycle with 200 μm and 500 μm medial-lateral displacement

The difference in contact pressure between applying the vertical loading magnitudes of F_y and F_1 was observed to be 18%, however the difference increased further when lateral edge loading boundary conditions were applied. To be consistent with experimental simulator testing methods, the range of lateral displacements were applied between the ranges of 200 μm and 500 μm, the results in Fig. 9 show the maximum contact pressure during a single ISO gait loading cycle with lateral microseparation applied throughout the loading cycle.

Results discussed above were based on a nominal cup inclination angle of 45°. By changing the inclination angle and anteversion angle, the effect on contact pressure and von Mises stress was assessed using the three-dimensional head and cup models without the backing of the pelvic and femur bones to obtain results with increased computational efficiency. The maximum contact pressure and von Mises stress at varying cup inclination angles and anteversion angles are provided in Fig. 10.

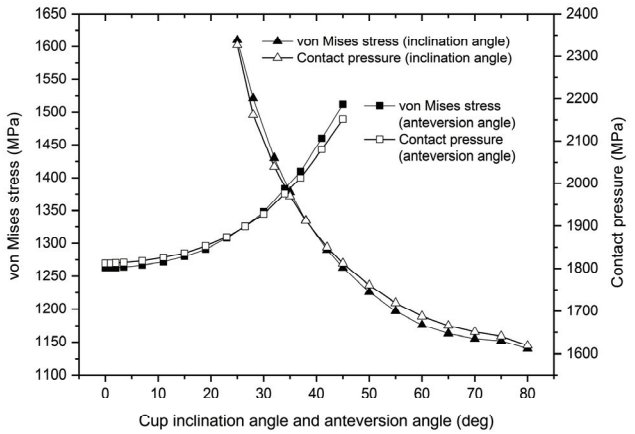

Fig. 10. Maximum contact pressure and von Mises stress against varying cup inclination angle and anteversion angle

The kinematics of "pure" microseparation was modelled to study laxity based edge loading of hip implants under contact. Following hip bearing microseparation, laxity of the hip joint is present as discussed in Section 2. By running an explicit model and applying a vertical load of 3900 N, relocation of the hip joint was observed whilst being able to assess the contact during this relocation analysis step. At a cup inclination angle of 45° contact initially occurred at the rim of the acetabular cup. The maximum contact pressure observed was 341 MPa and no contact was observed below the rim of the acetabular cup, i.e., the rim radius. When the cup inclination angle increased to 60° the maximum contact pressure increased to 646 MPa.

From the two-dimensional axisymmetric model, the maximum subsurface stresses were obtained for both the acetabular cup and femoral head components under F_1, F_y and F_s vertical loading conditions. The maximum stresses occurred below the surface of contact in all but one of the cases. It was only when a stumbling load was applied that the maximum stress occurred at the base of the head component. The maximum values of shear stress τ_{xy} and maximum σ_x, σ_y principal stress are provided in Table 2 and Table 3.

Table 2. Acetabular cup maximum stresses under vertical loads

Load	Max. shear stress (τ_{xy}) MPa	Principal stress (σ_x) MPa	Principal stress (σ_y) MPa
F_1	3.4	–19.8	–49.6
F_y	4.6	–25.5	–64.5
F_s	14.5	–69.6	–139.9

Table 3. Femoral head maximum stresses under vertical loads

Load	Max. shear stress (τ_{xy}) MPa	Principal stress (σ_x) MPa	Principal stress (σ_y) MPa
F_1	7.2	–37.1	–32.1
F_y	9.5	–49.7	–39.8
F_s	27.4	–135.2	–160.1

3.2. Wear simulations

The volumetric material loss due to mechanical wear under flexion-extension, internal-external rotation and ISO gait loading conditions were recorded for both the acetabular cup and femoral head simultaneously. By using the sliding distance algorithm method to determine the contact sliding distance and when applying a wear coefficient value (1.0×10^{-10} mm^3/Nm) to the wear model, the volumetric wear rates were 1.5 mm^3 per million cycles for the femoral head and 2.6 mm^3 per million cycles for the acetabular cup. A comparison between using the sliding distance output methodology and the coordinate output methodology was carried out. The difference in wear rates between using each method for the same segmented hip resurfacing model under angular displacement was 3.5% over one million cycles. For a wear simulation developed for 10 million cycles, the wear code was adapted to simulate and reflect long term wear, whilst considering the occurrence and trend of the wear observed experimentally. Achieving this result required the setup and development of a numerically stable model to manage the altering finite element mesh occurring during the wear simulations. A cumulative volumetric wear loss of material for both the femoral head and acetabular cup is presented in Fig. 11, as well as the

presentation of the volumetric wear loss of the femoral head against wear coefficient value over one million cycles (Fig. 12).

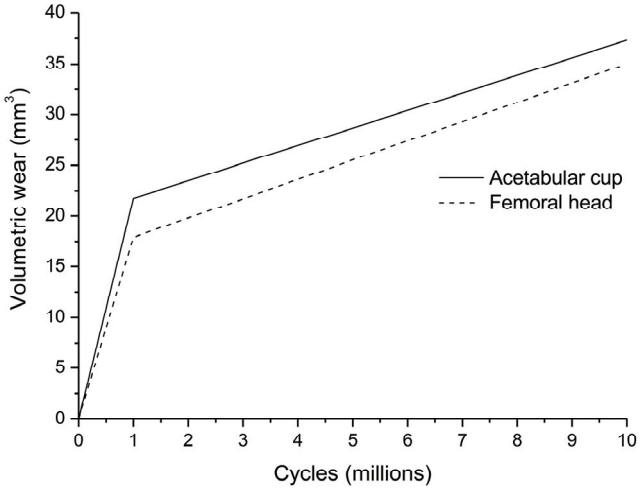

Fig. 11. Femoral head and acetabular cup volumetric wear over 10 million cycles

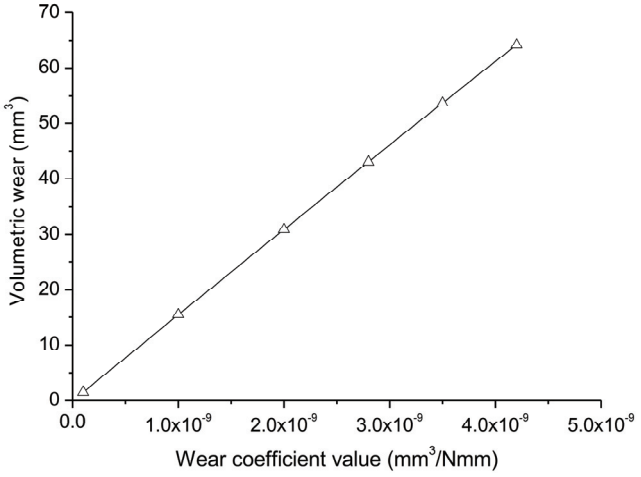

Fig. 12. Volumetric wear of the femoral head at different wear coefficient values

4. Discussion

The three-dimensional and two-dimensional hip resurfacing models have both provided unique and specific models for assessing the contact mechanics using a range of materials models and boundary conditions. By modelling bone material properties as isotropic, orthotropic and density based, it was determined that the contact pressure was insensitive to the intricacies associated with complex material models and relative differences in material models between the femur and pelvic bone sections. For low values of bone elastic modulus the principal stresses and von Mises stresses varied more greatly than the stress values at an elastic modulus greater than 5 GPa. The angular displacements and ISO loading conditions applied to the three-dimensional segmented model provided the option of calculating the sliding distances along with the application of variable loading using computational methods. The contact pressure between the femoral head and acetabular cup, as well as the shear stresses of these contact loadings matched the trend and profile of the input time dependant loading curve applied during the walking cycle.

By using the finite element method, the full range of lateral displacements typically applied during microseparation based hip simulator tests was modelled. The difference in maximum contact pressure observed when applying 200 μm and 500 μm was shown. Although ISO loading was applied, the contact between the bearing surfaces was dominated by edge loading due to the lateral displacement of the femoral head. This is shown by the contact pressure profile throughout the cycle not conforming the ISO gait loading profile.

The two-dimensional axisymmetric model allowed for an efficient assessment of the contact pressure and stresses at the surface and sub-surface of the bone and hip resurfacing implant devices. By applying the F_I, F_y and F_s vertical loads, increase in stresses were observed for both the femoral head and acetabular cup implant components as the vertical load increased.

A close comparison of sliding distance was obtained by using the two different sliding distance calculation methodologies, which provide an increased level of confidence in the validity of the wear results. Both methods provided a valid platform for assessing the volumetric wear between hip resurfacing devices using the finite element method with a custom scripting interface. The three-dimensional hip implant wear model provided volumetric wear results for both the acetabular cup and femoral head simultaneously, which has not been conducted before in previous studies. Although not compared extensively in previous studies, the results show the volumetric wear of the acetabular cup to be higher than for the femoral head which is also observed experimentally from cyclically simulated hip implant components [15]. A linear increase in volumetric wear was observed as the wear coefficient value increased, which shows the effect of the wear factor on the loss of material and highlights the importance for further study. The advantages of using the scripting method for developing hip implant wear simulations over previously published

methods using subroutine based simulations include less restrictions on element types and contact algorithms, as well as allowing an option for applying the wear model to both the acetabular cup and femoral head components simultaneously.

Overall, this study had demonstrated the use of computational and numerical methods for studying the contact mechanics of three-dimensional and two-dimensional axisymmetric hip resurfacing models. This was then extended to develop wear simulations to obtain the volumetric wear rates of hip implant devices under contact, angular displacement and variable loading conditions. This study has shown the possibility of using a Python scripting interface to simulate the volumetric wear loss by applying the Archard wear model to hip implants, and therefore model the long term performance of implant devices beyond current ISO standards for experimental simulator testing. This has been achieved whilst establishing the appropriate boundary conditions and material properties to be applied to the computational implant models. Further work includes longer term computational wear simulations with the inclusion of edge loading during the loading cycle.

Acknowledgements

This work was supported by the EPSRC (Engineering and Physical Sciences Research Council).

References

[1] LIU F., LESLIE I., WILLIAMS S., FISHER J., JIN Z., *Development of computational wear simulation of metal-on-metal hip resurfacing replacements*, Journal of Biomechanics, 2008, 41 (3), 686–694.

[2] MENG H., LUDEMA K., *Wear models and predictive equations: their form and content*, Wear, 1995, 181–183 (2), 443–457.

[3] ARCHARD J.F., *Contact and rubbing of flat surfaces*, Journal of Applied Physics, 1953, 24(8), 981–988.

[4] ROŃDA J., WOJNAROWSKI P., *Analysis of wear of polyethylene hip joint cup related to its positioning in patient's body*, Acta of Bioengineering and Biomechanics, 2013, 15(1).

[5] ALI M., MAO K., *Contact analysis of hip resurfacing devices under normal and edge loading conditions*, IAENG Special Issues Journal, 2012, 20(4), 317–329.

[6] ALI M., MAO K., *Modelling of hip resurfacing device contact under central and edge loading conditions*, Lecture Notes in Engineering and Computer Science Proceedings of The World Congress on Engineering, 2012, 20(4), 2054–2059.

[7] UDOFIA I.J., YEW A., JIN Z.M., *Contact mechanics analysis of metal-on-metal hip resurfacing prostheses*, Proceedings of the Institution of Mechanical Engineers Part H – Journal of Engineering in Medicine, 2004, 218, 293–305.

[8] SCHOLES S.C., UNSWORTH A., GOLDSMITH A.A.J., *A frictional study of total hip joint replacements*, Physics in Medicine and Biology, 2000, 45(12), 3721.

[9] BERGMANN G., GRAICHEN F., ROHLMANN A., BENDER A., HEINLEIN B., DUDA G., HELLER M., MORLOCK M., *Realistic loads for testing hip implants*, Bio-medical Materials & Engineering, 2010, 20(2), 65–75.

[10] HAREWOOD F., MCHUGH P., *Comparison of the implicit and explicit finite element methods using crystal plasticity*, Computational Materials Science, 2007, 39(2), 481–494.

[11] BERGMANN G., DEURETZBACHER G., HELLER M., GRAICHEN F., ROHLMANN A., STRAUSS J., DUDA G., *Hip contact forces and gait patterns from routine activities*, Journal of Biomechanics, 2001, 34(7), 859–871.

[12] FIRKINS P., TIPPER J., INGHAM E., STONE M., FARRAR R., FISHER J., *Influence of simulator kinematics on the wear of metal-on-metal hip prostheses*, Proceedings of the Institution of Mechanical Engineers, Part H, 2001, 215(1), 119–121.

[13] COUTEAU B., LABEY L., HOBATHO M.C., VANDER SLOTEN J., ARLAUD J.Y., BRIGNOLA J.C., *Validation of a three dimensional finite element model of a femur with a customized hip implant*, Computer Methods in Biomech. & Biomed. Eng., 1998, 1(1), 77–86.

[14] RHO J.Y., ASHMAN R.B., TURNER C.H., *Young's modulus of trabecular and cortical bone material: Ultrasonic and microtensile measurements*, Journal of Biomechanics, 1993, 26(2), 111–119.

[15] MANAKA M., CLARKE I.C., YAMAMOTO K., SHISHIDO T., GUSTAFSON A., IMAKIIRE A., *Stripe wear rates in alumina THR – Comparison of microseparation simulator study with retrieved implants*, Journal of Biomedical Materials Research Part B – Applied Biomaterials, 2004, 69(B), 149–157.